Can nutrient fertilization mitigate the effects of ozone exposure on an ozone-sensitive poplar clone?

Alessandra Podda[1(a, b)], Claudia Pisuttu[1(a)], Yasutomo Hoshika[(b)], Elisa Pellegrini[2 (a, c)], Elisa Carrari[(b)], Giacomo Lorenzini[(a, c)], Cristina Nali[(a, c)], Lorenzo Cotrozzi[(a)], Lu Zhang [(b, d)], Rita Baraldi[(e)], Luisa Neri[(e)], Elena Paoletti[(b)]

[(a)] Department of Agriculture, Food and Environment, University of Pisa, Via del Borghetto 80, Pisa, 56124, Italy

[(b)] Institute for Sustainable Plant Protection, National Research Council, Via Madonna del Piano 10, Sesto Fiorentino, Florence, 50019, Italy

[(c)] CIRSEC, Center for Climatic Change Impact, University of Pisa, Via del Borghetto 80, Pisa, 56124, Italy

[(d)] College of Horticulture and Landscape Architecture, Northeast Agricultural University, Changjiang Road 600, Harbin, 150030, China

[(e)] Institute of Biometeorology, National Research Council, Via P. Gobetti 101, Bologna, 40129, Italy

ABSTRACT

We tested the independent and interactive effects of nitrogen (N; 0 and 80 kg ha^{-1}), phosphorus (P; 0, 40 and 80 kg ha^{-1}), and ozone (O_3) application/exposure [ambient concentration (AA), 1.5 × AA and 2.0 × AA] for five consecutive months on biochemical traits of the O_3-sensitive Oxford poplar clone. Plants exposed to O_3 showed visible injury and an alteration of membrane integrity, as confirmed by the malondialdehyde by-product accumulation (+3 and +17% under 1.5 × AA and 2.0 × AA conditions, in comparison to AA). This was probably due to O_3-induced oxidative damage, as

[1] These authors have contributed equally to this work.
[2] Corresponding author.

documented by the production of superoxide anion radical ($O_2^{\bullet-}$, +27 and +63%, respectively). Ozone *per se*, independently from the concentrations, induced multiple signals (e.g. alteration of cellular redox state, increase of abscisic acid/indole-3-acetic acid ratio and reduction of proline content) that might be part of premature leaf senescence processes. By contrast, nutrient fertilization (both N and P) reduced reactive oxygen species accumulation (as confirmed by the decreased $O_2^{\bullet-}$ and hydrogen peroxide content), resulting in enhanced membrane stability. This was probably due to the simultaneous involvement of antioxidant compounds (e.g. carotenoids, ascorbate and glutathione) and osmoprotectants (e.g. proline) that regulate the detoxification processes of coping with oxidative stress by reducing the O_3 sensitivity of Oxford clone. These mitigation effects were effective only under AA and 1.5 × AA conditions. Nitrogen and P supply activated a free radical scavenging system that was not able to delay leaf senescence and mitigate the adverse effects of a general peroxidation due to the highest O_3 concentrations.

Keywords

Detoxification, oxidative damage, antioxidant compounds, nitrogen, phosphorus, premature senescence

1. Introduction

Tropospheric ozone (O_3) is widely recognised as the most damaging air pollutant to vegetation due to its broad geographical distribution and toxicity (Emberson et al., 2018). Ambient O_3 levels have often detrimental effects on crops and forests by inducing yield and biomass loss, and lowering plant resilience (Gao et al., 2017). Mineral nutrition can profoundly affect the O_3 sensitivity of woody plants (Maurer and Matyssek, 1997; Watanabe et al., 2012; Harmens et al., 2017). Mechanisms including alterations in growth and defence processes are still under debate (Shang et al., 2018). Some authors have reported that nutrient availability may determine the kind of plant

49 "strategy" useful to cope with O_3-induced oxidative stress, by driving leaf metabolic changes, such
50 as enhanced assimilation demand as a consequence of increased respiration rates and alteration in
51 carbohydrate partitioning (Pääkönen and Holopainen, 1995; Bielenberg et al., 2002; Harmens et al.,
52 2017). Other studies have suggested that nutrition may modify the responses to O_3 by shifts in
53 biomass allocation, which raise maintenance costs and accelerate leaf abscission (Pell et al., 1995;
54 Maurer and Matyssek, 1997; Watanabe et al., 2012). These discrepancies in the literature are
55 probably due to (i) species-specific responses, (ii) different experimental conditions (e.g., intensity
56 and duration of O_3 exposure), and (iii) management practices (e.g., fertilization regime, application
57 concentration and timing, and chemical form). In addition, studies on the interaction between O_3
58 sensitivity and soil nutrient conditions have mostly focused on traits such as visible injury,
59 photosynthetic capacity, biomass production and allocation, and leaf life-span (e.g., Maurer and
60 Matyssek, 1997; Singh et al. 2009; Harmens et al., 2017; Kinose et al., 2017a, b; Zhang et al.,
61 2018b), whereas biochemical investigations of the resulting oxidative stress and antioxidant defence
62 system in plants exposed to variable O_3 × nutrient conditions are lacking.

63 Proper levels of nitrogen (N) are necessary for plants to sustain a normal and consistent
64 growth (Barker and Bryson, 2007). This nutrient is the main component of enzymatic and structural
65 proteins, nucleic acids, chlorophylls and many secondary metabolites, and performs a vital role in
66 many metabolic processes (Epstein and Bloom, 2005). For example, N is an important component
67 of Rubisco, the enzyme that catalyses the initial steps of photosynthesis and changes inorganic
68 carbon to organic matter (LeBauer and Treseder, 2008). Nitrogen applications usually increase the
69 photosynthetic capacity which is commonly twinned with increased stomatal conductance (Zhang et
70 al., 2018b). Thus, N applications above the recommended doses can lead to an increased O_3 uptake
71 to levels at which antioxidant and repair mechanisms are no longer sufficient to counteract O_3-
72 induced oxidative damage (Harmens et al., 2017; Marzuoli et al., 2018).

73 Phosphorus (P) is the second most limiting nutrient for plant development and aboveground
74 net primary productivity of plants (Domingues et al., 2010). This macroelement is the main

component of several biomolecules such as phospholipids, sugar phosphates and nucleic acids that play a pivotal role in carbon metabolism, protein regulation and signal transduction (Amtmann and Blatt, 2009). Phosphorus deficiency alters the biochemistry of photosynthesis and increases sink demand for photosynthates for root growth, which in turn alters patterns of growth (Hernández and Munné-Bosch, 2015). Insufficient P availability leads to symptoms of photo-oxidative stress, such as increased free radical production and lipid peroxidation that are induced by disruptions in cellular homeostasis (Pintó-Marijuan and Munné-Bosch, 2014). Plants are able to activate a series of physiological, biochemical, and molecular adaptation strategies in order to increase nutrition uptake and recycling (Niu et al., 2012). These effects, however, could modify stomatal O_3 flux impairing the plant ability to compensate and counteract the negative impact of O_3 through detoxification and repair processes (Plaxton and Tran, 2011). To date, it is unclear how plants sense and respond to change in P availability under conditions of elevated O_3.

Poplar plantations are established in various soil nutritional conditions such as volcanic ash soils (low nutritional availability; Hoosbeek et al., 2004) and agricultural fields (high-nutritional availability; Arevalo et al., 2011). However, our knowledge of poplar responses to O_3 with various nutritional conditions is still limited.

In a previous work from the same experiment presented here, Zhang et al. (2018a) tested the independent and interactive effects of N, P and O_3 applications/exposure on biomass growth of the O_3-sensitive Oxford clone (*Populus maximoviczii* Henry × *Populus berolinensis* Dippel), showing that N addition exacerbated O_3-induced biomass loss, while P alleviated such biomass losses, but not under high N supply. However, no synergistic effects were found, suggesting an unbalance between avoidance (i.e., the ability of leaves to partially close stomata to exclude O_3 from leaf intercellular space) and repair strategies (i.e., the capacity to activate detoxifying systems).

The aim of the present study was to assess the nutritional impact on the metabolic adjustments adopted by Oxford clone to cope with three levels of O_3 in an O_3 Free Air Controlled Exposure (O_3-FACE) facility. Specifically, we asked the following questions: (i) What are the antioxidant

mechanisms activated in response to O_3? (ii) What are the cellular and metabolic rearrangements induced by different nutritional conditions? (iii) Can N and P availability trigger a set of adaptive responses to O_3? We postulated that nutrient availability can induce a cross-talk between antioxidant and osmotic mechanisms which regulate the strategy of coping with oxidative stress by reducing O_3 sensitivity.

2. Materials and Methods

2.1. Plant material and experimental design

The experimental activities were conducted in an O_3-FACE system located in Sesto Fiorentino, Italy (43° 48' 59" N, 11° 12' 01" E, 55 m a.s.l.) as described in Paoletti et al. (2017). Rooted homogeneous cuttings of Oxford clone were propagated in a greenhouse in early December 2015 and transferred to the O_3-FACE facility in April 2016, where they were transplanted into individual 10-L plastic pots containing a mixture of sand:peat:soil (1:1:1 in volume). Plants were irrigated to field capacity every 2-3 days to avoid water stress. Uniform-sized plants were selected and exposed to one of these three levels of O_3: ambient air concentration (AA), 1.5 × AA, and 2.0 × AA, and subjected to six combinations of nutrient treatment, i.e. two levels of N (0 and 80 kg N ha^{-1}; N0 and N80, respectively) and three levels of P (0, 40 and 80 kg P ha^{-1}; P0, P40 and P80, respectively)] from 1st May to 1st October, 2016. The Accumulated Ozone exposure over a Threshold of 40 ppb (AOT40, sensu Kärenlampi and Skärby, 1996) were 14.4, 43.8 and 71.1 ppm h in AA, 1.5 × AA and 2.0 × AA, respectively, throughout the experimental period (the average concentrations of O_3 were 35±0.3, 51.6±0.5 and 66.7±0.5 ppb, respectively). A detailed description of the O_3 exposure methodology and nutritional treatments is available in Zhang et al. (2018a). The N and P amounts provided in the present study were higher than the nutrient inputs occurring in European forests (Ferretti et al., 2014). However, the level of N80 may be considered as a realistic N deposition because the background deposition in some areas, such as the Sichuan basin in China and the California Central Valley in USA, may be higher than 80 kg N ha^{-1} yr^{-1} (Zhang et al., 2018b),

126 whereas P levels were selected based on P affinity constant and adsorption maxima to simulate a
127 realistic increase in soil available P. Nitrogen deposition in Italy has been reported as ranging
128 between 7 and 24 kg N ha^{-1} yr^{-1} in Italy, mainly due to wet deposition (Ferretti et al., 2014). Plants
129 received approximately one-third of the annual value of precipitation (227 mm) during the
130 experimental period. So we may say that they received approximately 2-8 kg N ha^{-1} by rainfall. The
131 soil N and P concentrations were shown in our previous paper (Zhang et al. 2018a). Soil N
132 concentration (mean±S.E.) in N0 was 1.7±0.1 g kg^{-1}, and that in N80 was 2.7±0.1 g kg^{-1}. These
133 values are in agreement with normal soil N ranges (0.2 to 5 g kg^{-1}, Bowen 1979). Soil P
134 concentrations (mean±S.E.) were 0.5±0.1 g kg^{-1} in P0 and 1.0±0.1 g kg^{-1} in P80, i.e. within the
135 range of native P in soils (usually 0.5 to 0.8 g kg^{-1}, with peaks of 1.0 to 1.3 g kg^{-1}, Stevenson and
136 Cole 1999). Three replicated plots (5 × 5 × 2 m) were assigned to each O_3 treatment, with three
137 plants per each combination of O_3 level, and N and P enrichment. Plants were repositioned every
138 month within each plot to avoid positional effects (Potvin and Tardif, 1988). At the end of the
139 experiment, fully expanded leaves (5^{th}-8^{th} order from the tip terminal shoot, flushed in July 2016) of
140 all the three plants per plot in each O_3 × N × P treatment were gathered (from 9:00 to 12:00 am),
141 divided into aliquots, immediately frozen in liquid nitrogen and stored at -80 °C until biochemical
142 analyses. Biochemical analyses aimed to investigate the O_3-induced oxidative damage [i.e., lipid
143 peroxidation and reactive oxygen species (ROS) contents] as well as the antioxidative (i.e., foliar
144 pigments, ascorbate and glutathione) and osmoprotective [i.e., proline (Pro), abscisic acid (ABA),
145 indole-3-acetic acid (IAA) and water soluble carbohydrates (WSC)] responses adopted by poplar
146 under variable environments. Leaf mass per area (LMA) was not different between the treatments
147 and the mean value (mean±S.E.) was 75.5±1.5 g m^{-2}.

148 *2.2. Visible injury, oxidative damage and ROS content*

149 Leaf injury was evaluated every month to determine the percentage of injured area on the adaxial
150 surface by in-hand examination with a 10× hand lens with the help of photoguides (Paoletti et al.,

2009). All fully expanded attached leaves per each plant were examined. The percentage of affected leaves per plant (LA), and the 5%-step percentage of area affected in the symptomatic leaves (AA) were visually scored, and a Plant Injury Index (PII) was calculated combining the two parameters: PII = (LA × AA)/100 (Paoletti et al., 2009).

Lipid peroxidation was estimated by determining the malondialdehyde (MDA) by-product accumulation, according to the method of Hodges et al. (1999) with minor modifications, as reported by Guidi et al. (2017). The determination was performed with a fluorescence/absorbance microplate reader (Victor3 1420 Multilabel Counter, Perkin Elmer, Waltham, MA, USA).

Superoxide anion radical ($O_2^{\bullet-}$) content was measured according to Tonelli et al. (2015) with the same fluorescence/absorbance microplate reader reported above. This assay is based on the reduction of a tetrazolium dye sodium, 3'-(1-[phenylamino-carbonyl]-3,4-tetrazolium)-bis(4-methoxy-6-nitro) benzene-sulfonic acid hydrate (XTT) by O_2 to a soluble XTT formazan (Able et al., 1998).

Hydrogen peroxide (H_2O_2) content was measured using the Amplex Red Hydrogen Peroxide/Peroxidase Assay Kit (Molecular Probes, Life Technologies Corp., Carlsbad, CA, USA) according to Cotrozzi et al. (2017a). The determination was performed with the same fluorescence/absorbance microplate reader reported above at 510 and 590 nm (excitation and emission of resofurin fluorescence, respectively).

2.3 Non-enzymatic antioxidant compounds

Photosynthetic and accessory pigments were measured after extracting 30 mg of leaf tissue in 0.3 mL of 100% HPLC-grade methanol overnight at 4 °C in the dark. Pigments were then determined by High Performance Liquid Chromatography (HPLC; P680 Pump, UVD170U UV-VIS detector, Dionex, Sunnyvale, CA, USA) at room temperature with a reverse-phase Dionex column (Acclaim 120, C18, 5 µm particle size, 4.6 mm internal diameter × 150 mm length), according to Cotrozzi et

al. (2017b), with some minor modifications. Samples were centrifuged for 15 min at 16,000 *g* at 5 °C and the supernatant was filtered through 0.2 μm Minisart® SRT 15 aseptic filters and immediately analyzed. The pigments were eluted using 100% solvent A (acetonitrile/methanol, 75/25, v/v) for the first 14 min to elute all xanthophylls, followed by a 1.5 min linear gradient to 100% solvent B (methanol/ethylacetate, 68/32, v/v), 15 min with 100% solvent B, which was pumped for 14.5 min to elute chlorophyll (chl) *b* and *a* and β-carotene, followed by 2 min linear gradient to 100% solvent A. The flow-rate was 1 mL min^{-1}. The column was allowed to re-equilibrate in 100% solvent A for 10 min before the next injection. The pigments were detected by their absorbance at 445 nm. To quantify the pigment content of each sample, known amounts of pure authentic standards were injected into the HPLC system and an equation, correlating peak area to pigment concentration, was formulated. The data were evaluated by Dionex Chromeleon software, according to the manufactor.

Reduced (AsA) and oxidized (DHA) ascorbate contents were measured according to the method of Kampfenkel et al. (1995). This assay is based on the reduction of ferric ions (Fe^{3+}) to ferrous ions (Fe^{2+}) with ascorbic acid in acid solution, followed by the formation of the red chelate between Fe^{2+} ions and 2,2-dipyrydil. Samples were ground with mortar and pestle and then extracted with 1 mL of 6% (w/v) trichloroacetic acid. Total ascorbate (AsA + DHA) was determined through a reduction of dehydroascorbate to ascorbate by dithiothreitol. DHA concentrations were estimated from the difference between amounts of total ascorbate and AsA. The determination was performed with a spectrophotometer (6505 UV-Vis, Jenway, Staffordshire, UK) at 525 nm.

Reduced (GSH) and oxidized (GSSG) glutathione contents were measured according to the method of Griffith (1980). This assay is based on an enzymatic recycling procedure in which glutathione was sequentially oxidized by 5,5'-dithiobis-2-nitrobenzoic acid and reduced by NADPH in the presence of glutathione reductase. Samples were added to 0.5 mL 6% (w/v) trichloroacetic acid. For specific assay of GSSG, GSH was masked by derivatization with 4-vinylpyridine in the

presence of triethanolamine. Changes in absorbance of the reaction mixtures were measured at 412 nm for 15 min at 25 °C. The amount of GSH was calculated by subtracting the GSSG amount, as GSH equivalents, from the total glutathione amount. A standard calibration curve, where GSH equivalents (from 0 to 10 mM) were plotted against the slope of change in absorbance at 412 nm, was used.

2.4. Osmoprotective compounds

Pro content was measured according to the procedure described by Cotrozzi et al. (2017b), which is based on the colorimetric reaction of Pro with ninhydrin (Bates et al., 1973). The determination was performed at 520 nm with the same spectrophotometer reported above.

The content of the free forms of both IAA and ABA were analysed according to Ludwig-Müller et al. (2008) and Brilli et al. (2018), with some modifications. Approximately 0.02 g dry weight (DW) of lyophilized leaf material were extracted with 1 mL isopropanol:acetic acid (95:5, v/v), to which 500 ng each of $^{13}C_6$-IAA and $^{2}H_6$-ABA (OlChemIm, Olomouc, Czech Republic) were added as internal standards for quantitative mass-spectral analysis. After overnight isotope equilibration at 4 °C, the samples were centrifuged for 10 min at 10,000 *g*, the supernatants were collected and, after a double re-extraction of the pellet with 500 µL extraction solution, were evaporated to dryness with a rotary evaporator. The residues were resuspended in 300 µL methanol and methylated with 500 µL diazomethane in the dark for about 30 min, then dried under a gentle N_2 gas stream (Baraldi et al., 1988). The samples were finally resuspended in 30 µL ethyl acetate and 2 µL were injected into a GC-MS system (7890A-5975C, Agilent Technologies, Santa Clara, CA, USA) in splitless mode onto a HP1 capillary column (length 60 m, inner diameter 0.25 mm; film thickness 0.25 µm, Agilent Technologies, Santa Clara, CA, USA). Helium was employed as a carrier gas and provided at a flow rate of 1 mL min^{-1}, GC injector was set at 280 °C and the oven temperature was increased from 90 to 200 °C at a rate of 20 °C min^{-1}, then at a rate of 8 °C min^{-1} until 280 °C, followed by 4 min isotermically at 280 °C. The source temperature was set at 230 °C

and ionizing voltage was 70 eV. Ions monitored were: m/z 130, 136 for the base peak (quinolinium ion) and m/z 189, 195 for the molecular ion of the methyl-IAA and the methyl-$^{13}C_6$-IAA, respectively; m/z 190, 194 for the base peak and m/z 162, 166 for the molecular ion of the methyl-ABA and methyl-$^{2}H_6$-ABA, respectively. For absolute quantification, the endogenous hormone levels were estimated from the corresponding peak area by calculating the ratios between m/z 130/136 and m/z 189/195 for IAA, and m/z 190/194 and 162/166 for ABA, according to the principles of isotope dilution (Cohen et al. 1986).

WSC were measured after extracting 60 mg of leaf tissue in 1 mL of demineralized water for HPLC and heating for 60 min in a water bath at 60 °C. The extracts were analyzed by HPLC (with the same pumps used for photosynthetic pigments) equipped with a BioRad column (Aminex HPX-87H, 300 × 7.8 mm, Richmond, CA, USA) at 50 °C, according to Pellegrini et al. (2015) with some minor modifications. Samples were centrifuged for 20 min at 5,000 *g* at 20 °C and the supernatant was filtered through 0.2 μm Minisart® SRT 15 aseptic filters and immediately analyzed. The carbohydrates were detected with a differential refractometer (Shodex, West Berlin, NJ, USA) and demineralized water for HPLC was used as mobile phase (flow rate 0.8 mL min^{-1}). To quantify the carbohydrate content of each sample, known amounts of pure authentic standards were injected into the HPLC system and an equation, correlating peak area to WSC concentration, was formulated.

2.5. Statistical analysis

Statistical analyses were performed with JMP 11.0 (SAS Institute, Cary, NC, USA). The study was conducted in a well-replicated split-plot experiment with a full-factorial combination of treatments. Ozone was the whole-plot factor as each of the three O_3 levels had three blocks and the six nutrient combinations (two levels of N and three levels of P) were randomly assigned to 18 pots (three pots per nutrient combination), distributed among the three blocks of each O_3 level (for a total of 54 pots distributed among nine blocks). All data were tested with Kolmogorov-Smirnov test for normality and with Levene test for homogeneity of variance. All data were normally distributed and thus were

analyzed with a full-factorial split-plot three-way analysis of variance (ANOVA) with O_3, N and P as fixed factors, and the block as random factor nested in O_3. Differences ($P \leq 0.05$) were tested by Tukey's HSD post-hoc test. The statistical unit was the single pot (N = 3).

3. Results

3.1. Visible injury, oxidative damage and ROS content

Plants exposed to O_3 (alone or in combination with N and/or P treatments) developed visible minute stipples of browning tissue localized in the interveinal adaxial leaf area. The most severe damage occurred in 2.0 × AA_N0_P0 plants (Table 1): 42% of the scored leaves were affected, and the injured leaves had on average 20% of their surface covered by stippling. Nitrogen enrichment *per se* decreased PII when the N80_P0 treatment was compared to the N0_P0 only under 1.5 × AA and 2.0 × AA O_3 concentrations (-61 and -70%, respectively). Phosphorus enrichment *per se* decreased PII values relative to N0_P0 (independently of O_3 concentrations), with significant differences between the P treatments only under 1.5 × AA conditions (-46 and -68% in P40 and P80, respectively). Increased PII values were observed when N and P enrichments were combined, under 2.0 × AA conditions, with significant differences between the P treatments (about two-fold higher than N80_P0).

The three-way ANOVA showed that all the effects on MDA, $O_2^{\bullet-}$ and H_2O_2 were significant, except for N enrichment on $O_2^{\bullet-}$ (Table 2). Compared to AA_N0_P0 conditions, MDA was (i) increased by O_3 *per se*, with significant differences between the two higher O_3 concentrations (+3 and +17% in 1.5 × AA and 2.0 × AA, respectively; Fig. 1); (ii) markedly decreased by N enrichment *per se* (-36%), and (iii) decreased by P enrichment *per se*, with significant differences between the P treatments (-19 and -9% in P40 and P80, respectively). Under combined O_3 and N enrichment conditions, MDA significantly decreased when all N80_P0 treatments were compared to N0_P0 ones, independently of O_3 concentrations. Unchanged MDA values were observed when

N and high P enrichments were combined under 1.5 × AA and 2.0 × AA conditions. By contrast, the combination of O_3 and P enrichment induced a marked decrease of MDA, independently of the level of both factors.

Compared to AA_N0_P0 conditions, $O_2^{\bullet-}$ was (i) increased by O_3 *per se*, with significant differences between the two higher O_3 concentrations (+27 and +63% in 1.5 × AA and 2.0 × AA, respectively; Fig. 2); (ii) slightly decreased by N enrichment *per se* (-12%), and (iii) unchanged by P enrichment *per se*. Under combined O_3 and N enrichment conditions, $O_2^{\bullet-}$ content significantly decreased when N80_P0 treatment was compared to N0_P0, only under 2.0 × AA conditions. By contrast, the combination of N and P enrichment induced a marked increase of $O_2^{\bullet-}$ in comparison to N80_P0, independently of O_3 concentrations (except in the case of 1.5 × AA_N80_P40). Unchanged $O_2^{\bullet-}$ values were observed when O_3 and high P enrichments were combined compared to N0_P0 (except in the case of 1.5 × AA).

Compared to AA_N0_P0 conditions, H_2O_2 was (i) increased by moderate O_3 concentrations *per se* (+4%, Fig. 3); (ii) significantly decreased by N enrichment *per se* (-56%), and (iii) decreased by high P enrichment *per se* (-42%). Under combined O_3 and N enrichment conditions, H_2O_2 content significantly decreased when all N80_P0 treatments were compared to N0_P0, independently of O_3 concentrations (except under 1.5 × AA conditions). By contrast, the combination of N and P enrichment induced a marked increase of H_2O_2 compared to N80_P0, independently of O_3 concentrations (except in the case of 1.5 × AA_N80_P40). Compared to N0_P0 conditions, reduced H_2O_2 values were observed when O_3 and P enrichments were combined under 1.5 × AA (except in the case of 1.5 × AA_N0_P80) and 2.0 × AA conditions.

3.2. Non-enzymatic antioxidant compounds

The three-way ANOVA showed that all the effects on Tot Car, AsA/DHA and GSH/GSSG ratio were significant (Table 2). Compared to AA_N0_P0 conditions, Tot Car content was (i) increased

by high O_3 concentrations *per se* (+60%, Fig. 4); (ii) slightly decreased by N enrichment *per se* in leaves grown under AA_N80_P0 conditions (-36%), and (iii) unchanged by P enrichment *per se*. Under combined O_3 and N enrichment conditions, Tot Car content significantly decreased when N80_P0 treatments were compared to N0_P0, only under 2.0 × AA conditions (-23%). Similarly, the combination of N and P enrichment induced a marked decrease of Tot Car content compared to N80_P0 under 2.0 × AA conditions (without significant differences between P concentrations). Compared to N0_P0, a decrease of Tot Car content was observed when moderate O_3 and high P enrichments were combined (-24%). The same response was observed when high O_3 and P enrichments were combined, with significant differences between P concentrations.

Compared to AA_N0_P0 conditions, AsA/DHA ratio was increased by moderate O_3 concentrations *per se* (+19%) and P enrichment *per se*, without significant differences between P concentrations (Fig. 5). Under combined O_3 and N enrichment conditions, the AsA/DHA ratio significantly increased when all N80_P0 treatments were compared to N0_P0, only under 2.0 × AA conditions. Similarly, the combination of N and P enrichment induced a marked decrease of AsA/DHA ratio compared to N80_P0, under AA and 2.0 × AA conditions (with significant differences between P concentrations under AA conditions). A decrease of AsA/DHA ratio was observed when moderate O_3 concentrations and P enrichments were combined compared to N0_P0, with significant differences between P concentrations (-11 and -44%, in P40 and P80, respectively).

Compared to AA_N0_P0 conditions, GSH/GSSG ratio was only altered by O_3 *per se* (-52 and +56% by O_3 concentrations, under 1.5 × AA and 2.0 × AA conditions, respectively, Fig. 6). Under combined O_3 and N enrichment conditions, the GSH/GSSG ratio significantly decreased when N80_P0 treatments were compared to N0_P0, only under 2.0 × AA conditions. The combination of N and P enrichment induced a marked increase of GSH/GSSG ratio compared to N80_P0, under AA and 2.0 × AA conditions (with significant differences between P concentrations under 2.0 × AA

conditions). An increase of GSH/GSSG ratio was observed when the two higher O_3 concentrations and P enrichment were combined compared to N0_P0 (except in the case of 2.0 × AA_N0_P80).

3.3. Osmoprotective compounds

The three-way ANOVA showed that all the effects on Pro, abscisic acid/indole-3-acetic acid ratio (ABA/IAA) and WSC were significant, except for P enrichment on ABA/IAA ratio (Table 2). Proline was increased by each single factor (+40, +21 and around +23% by high O_3 concentrations, N and P enrichment *per se*, respectively, Fig. 7). Under combined O_3 and N enrichment conditions, Pro significantly increased when all N80_P0 treatments were compared to N0_P0, except under high O_3 concentrations. Similarly, the combination of N and P enrichment induced a marked increase of Pro compared to N0_P0, in 1.5 × AA and 2.0 × AA conditions (except in the case of 2.0 × AA_N80_P40). Increased Pro values were observed when O_3 and P enrichments were combined compared to N0_P0, independently of O_3 and P concentrations (except in the case of 1.5 ×AA_N0_P40).

Compared to AA_N0_P0 conditions, ABA/IAA was not altered by each factor *per se* (Fig. 8). Only the combination of N and P enrichment induced a marked decrease of ABA/IAA compared to N80_P0 under 1.5 ×AA conditions. Compared to N0_P0 conditions, increased ABA/IAA values were observed when moderate O_3 concentrations and moderate P enrichment were combined.

Compared to AA_N0_P0 conditions, WSC was (i) increased by high O_3 concentrations *per se* (+32%, Fig. 9); (ii) markedly decreased by N enrichment *per se* in leaves grown under AA_N80_P0 conditions (-36%), and (iii) unchanged by P enrichment *per se*. Under combined O_3 and N enrichment conditions, WSC significantly decreased when all N80_P0 treatments were compared to N0_P0, independently of O_3 concentrations. By contrast, the combination of N and high P enrichment induced a marked increase of WSC compared to N80_P0, only under 2.0 × AA

conditions. Unchanged WSC values were observed when increased O_3 concentrations and high P enrichments were combined relative to N0_P0.

Discussion

To ensure their survival, plants have to cope with a variety of environmental constraints such as O_3 and nutrient availability (Landolt et al., 1997). It is well known that O_3 exposure causes both visible and physiological damage to trees (Pellegrini et al., 2011, 2018; Cotrozzi et al., 2016; Zhang et al., 2018b). Visible injury is often a marker of O_3-induced oxidative damage, although it does not always coincide with an alteration of the photosynthetic performance (Paoletti et al., 2009; Gottardini et al., 2014; Yang et al., 2016). Ozone sensitivity of several species and clones of the genus *Populus* has been documented (Lorenzini et al. 1999; Pellegrini et al., 2012). This sensitivity is attributed to the high stomatal conductance, that is typical of fast-growing tree species (Marzuoli et al., 2008). Foliar injuries in the O_3-sensitive Oxford poplar clone have been detected in previous open-top chamber experiments, suggesting that an unbalance between avoidance (i.e. the ability of leaves to partially close stomata to exclude O_3 from leaf intercellular space) and repair strategies (i.e. the capacity to activate detoxification systems) occurred (Marzuoli et al., 2008). In our previous work (Zhang et al., 2018a), we confirmed that N enrichment increased O_3 uptake by 5-10%, while P reduced it by 4-10% in Oxford poplar clone. Although P enrichment slightly decreased O_3 uptake, we did not find significant mitigation effects of P on O_3-induced biomass reduction. On the other hand, the interactive effects of O_3 × N on biomass were statistically significant. As a result, in both cases of AOT40 and Phytotoxic Ozone Dose 4, we found the greater reduction of biomass per unit O_3 uptake under N enrichment compared to N0, suggesting that N increased the O_3 sensitivity. Such sensitivity is probably closely related to repair and detoxification processes.

In light of the above, the first question we wanted to address was “What are the antioxidant mechanisms activated by poplar in response to O_3?”. In a previous work from the same experiment

371 presented here, Zhang et al. (2018b) focused on the independent and interactive effects of N, P and
372 O_3 applications/exposure on ecophysiological traits of Oxford clone, and reported that plants
373 exposed to the two higher O_3 concentrations showed accelerated leaf senescence and a significant
374 decrease of photosynthetic efficiency. Here, our results confirm that visible injury and membrane
375 damage occurred (i.e. pronounced increase of MDA by-product values), likely due to an O_3-induced
376 oxidative burst, as documented by H_2O_2 and $O_2^{\bullet-}$ accumulation. The alteration of membrane
377 structure and integrity under increased ROS conditions are characteristic of O_3-sensitive plants,
378 which are not able to defend themselves through metabolic adjustments (Rao et al., 2000). Our
379 results suggest that the two higher O_3 concentrations modified the redox state of the metabolites
380 involved in the Halliwell-Asada cycle, although in a different way between the O_3 levels. Under 1.5
381 × AA conditions, enhanced ROS evolution had a lower impact on the AsA/DHA ratio than on the
382 GSH/GSSG ratio, suggesting that GSH turnover was probably necessary to sustain the conversion
383 of DHA to AsA in leaf tissue, where an extra amount of reducing power is available due to limited
384 CO_2 assimilation (Polle, 1996). Under 2.0 × AA conditions, an opposite trend was observed,
385 suggesting that AsA pool could be directly involved in O_3-derived ROS scavenging at this O_3
386 concentration, as indicated by the low AsA/DHA ratio. These results confirm that AsA represents
387 the first line of defence against O_3-induced oxidative load (Noctor and Foyer, 1998), although it
388 does not seem sufficient to mitigate the negative effects of O_3 in terms of ROS production and
389 membrane denaturation (van Hove et al., 2001). According to Foyer and Noctor (2011), it is
390 possible to speculate that intracellular AsA was more important in terms of regulation than in redox
391 homeostasis. This is probably because AsA is a cofactor of several plant-specific enzymes that are
392 involved in important pathways leading to the biosynthesis of (i) plant hormones (e.g. ABA), (ii)
393 defence-related secondary metabolites and (iii) cell wall hydroxyproline-rich proteins (Gest et al.,
394 2013). Our results suggest that the two higher O_3 concentrations induced multiple signals that might
395 be a part of a premature leaf senescence process, although in a different way between the O_3 levels.
396 Under 1.5 × AA conditions, the observed increase of ABA/IAA ratio and the concomitant reduction

of Pro content indicate that these compounds triggered a premature leaf death rather than an osmoregulation (Cotrozzi et al., 2016). Under 2.0 × AA conditions, plants showed an interaction among ABA/IAA, Pro and WSC resulting in an orchestrated signalling response that might be part of a premature leaf senescence process (Cotrozzi et al., 2017b). These results confirm that plants were not able to adopt metabolic adjustments in order to activate repair strategies against the two higher O_3 concentrations.

In light of the above, the second question was "What are the cellular and metabolic rearrangements induced by different nutritional conditions in poplar?". It is known that N fertilization, applied in a broad range of doses, has positive effects on plant growth (Wooliver et al., 2017), biomass production (Neuberg et al., 2010) and photosynthetic performance (Shang et al., 2018; Zhang et al., 2018b). In our study, the availability of N was effective in lowering ROS accumulation (as confirmed by the decrease of H_2O_2 and $O_2^{\bullet-}$ content), resulting in enhanced membrane stability (e.g. reduced and/or unchanged PII values), independently to O_3 concentrations. This is probably due to simultaneous involvement of antioxidant compounds (e.g. Car and AsA) and osmoprotectants (e.g. Pro and WSC) that are crucial for preventing oxidative damage (Sharma et al., 2012; Pellegrini et al., 2016). Nitrogen treatment *per se* induced a reduction of Tot Car (except under 1.5 × AA conditions) and an alteration of cellular redox state (e.g. changed AsA/DHA and GSH/GSSH ratio) confirming that these antioxidants could be consumed by the cell to prevent and/or scavenge the possible ROS generation (Gill and Tuteja, 2010). In addition, N treatment *per se* was beneficial by diverting photosynthates from the formation of transport or storage carbohydrates (as confirmed by the decrease of WSC content) toward amino acid synthesis, as reported by Champigny and Foyer (1992). In particular, the observed stimulation of Pro biosynthesis could have contributed to (i) sustain the electron flow between photosystems, (ii) enhance membrane stability, (iii) reduce damage of the photosynthetic apparatus, and (iv) stabilize key enzymes, such as Rubisco (Szabados and Savouré, 2010).

Phosphorus is another essential element for plant growth and development. It plays crucial roles in energy transfer, signal transduction, photosynthesis, regulation of metabolic pathways, membrane synthesis and stability, and respiration (Chiou and Lin, 2011). Similarly to N, the availability of P enhanced membrane stability by keeping ROS under control (except $O_2^{\bullet-}$ and H_2O_2 in the case of AA_N0_P40 and 1.5 × AA_N0_P80), independently to O_3 concentrations, as confirmed by the reduced and/or unchanged PII values. This result suggests that an activation of an efficient free radical scavenging system prevented the oxidative damage. In particular, P treatment *per se* induced an alteration of cellular redox state (e.g. changed AsA/DHA and GSH/GSSH ratio) and an increase of Pro content (except in the case of 1.5 × AA_N0_P40) confirming that these antioxidants could regulate the level of ROS in order to prevent the occurrence of the oxidative load (Gill and Tuteja, 2010). These results confirm that nutrient availability (N supply or increasing P concentrations) induced several cellular and metabolic rearrangements in order to enhance the defense capability of plants, according to Cao et al. (2016).

Finally, the third question was "Can N and P availability trigger a set of plant adaptive responses to O_3?". The role of nutrition in O_3 tolerance is rather uncertain, and information on this topic is scarce (Landolt et al., 1997). In particular, studies have been conducted in order to evaluate the possible role of nutrient availability as modifier of O_3-induced effects at physiological level (Maurer and Matyssek, 1997; Utrianen and Holopainen, 2001; Zhang et al., 2018a, b). As reported before, N supply, as well as increasing P concentrations, had a positive effect by enhancing the ability of cells to scavenge O_3-derived ROS. This result suggests that nutrient availability triggers a set of adaptive responses to O_3. In our study, N and P treatments induced an important remobilization of amino acids (e.g. Pro) in response to O_3 (independently of the concentrations), in order to provide energy and antioxidants to limit negative effects (Dumont et al., 2014). In addition, the concomitant synthesis and/or regeneration of the metabolites involved in the Halliwell-Asada cycle contributed to mitigate and/or limit the damage caused by O_3, as confirmed by the reduced or

447 unchanged PII values and the enhanced membrane stability. However, these mitigation effects
448 appeared to be effective only under AA and 1.5 × AA conditions. N and P supply activated a free
449 radical scavenging system that was not able to delay leaf senescence and minimize the adverse
450 effects of a general peroxidation due to the higher O_3 concentrations. This is consistent with the
451 finding in Zhang et al. (2018b). In fact, Zhang et al. (2018b) reported that O_3-induced loss of net
452 photosynthesis was mitigated by N enrichment under 1.5 × AA conditions. However, such a
453 mitigation effect was not found under 2.0 × AA conditions. Nitrogen addition exacerbated O_3-
454 induced increase of dark respiration rate suggesting an increased respiratory carbon loss in the
455 presence of O_3 and N. This may result in a further reduction of the net carbon gain for plants
456 exposed to O_3.

457 In conclusion, nutrient availability induced a cross-talk between antioxidant and osmotic
458 mechanisms which regulated the detoxification and/or repair processes of coping with oxidative
459 stress, by reducing O_3 sensitivity of Oxford clone grown under AA and 1.5 × AA conditions. The
460 present study, together with the ones by Zhang et al. (2018a,b), represents an important and wide-
461 ranging investigation of the interactive effects of nutrient conditions on the O_3 sensitivity of poplar.
462 However, further studies on the nutrient-O_3 sensitivity interaction are needed to estimate the impact
463 of the environmental changes on plants, given the potential and expected specificity of the
464 investigated responses for (i) the tested species (we used an O_3-sensitive poplar clone), (ii) the
465 experimental conditions such as the intensity and duration of O_3 exposure or the plant age (we used
466 young potted plants), and (iii) the management practices such as fertilization regime, application
467 concentration and timing (we used high N and P amounts applied only for five months).

468 **Acknowledgments**

469 We are thankful to Dr. Giuseppe Conte and Dr. Yutaka Osada for the critical review of the
470 statistical analysis. The authors wish to thank the five anonymous peer reviewers for their

constructive comments, suggestions and criticisms, which helped to substantially improve and clarify an earlier draft of the manuscript.

References

Able, A.J., Guest, D.I., Sutherland, M.W., 1998. Use of a new tetrazolium-based assay to study the production of superoxide radicals by tobacco cell cultures challenged with avirulent zoospores of *Phytophthora parasitica* var. *nicotianae*. Plant Physiol. 117, 491-499.

Amtmann, A., and Blatt, M.R., 2009. Regulation of macronutrient transport. New Phytol. 181, 35-52.

Arevalo, B.M., Bhatti, J., Chang, S.X., Sidders, D., 2011. Land use change effects on ecosystem carbon balance: From agricultural to hybrid poplar plantations. Agric. Ecosyst. Environ. 141, 342-349.

Baraldi, R., Chen, K.H., Cohen, J.D., 1988. Microscale isolation technique for quantitative gas chromatography-mass spectrometry analysis of indole-3-acetic acid from cherry (*Prunus cerasus* L.). J. Chrom. 44, 301-306.

Barker, A.V., and Bryson, G.M., 2007. Nitrogen. In: A.V. Barker and D.J. Pilbeam (Eds.), Handbook of plant nutrition, Taylor & Francis, New York , pp. 21-50.

Bates, L., Waldren, R.P., Teare, I.D., 1973. Rapid determination of free proline for water-stress studies. Plant Soil, 39, 205-207.

Bielenberg, D.G., Lynch, J.P., Pell, E.J., 2002. Nitrogen dynamics during O_3-induced accelerated senescence in hybrid poplar. Plant Cell Environ. 25, 501-512.

Bowen, H.J.M., 1979. Environmental chemistry of the elements. London: Academic Press.

Brilli, F., Pollastri, S., Raio, A., Baraldi, R., Neri, L., Bartolini, P., Podda, A., Loreto, F., Maserti, B.E., Balestrini, R., 2018. Root colonization by *Pseudomonas chlororaphis* primes tomato (*Lycopersicum esculentum*) plants for enhanced tolerance to water stress. J. Plant Physiol. doi:10.1016/j.jplph.2018.10.029.

Cao, J.X., Shang, H., Chen, Z., Tian, Y., Yu, H., 2016. Effects of elevated ozone on stoichiometry and nutrient pools of *Phoebe bournei* (Hemsl.) Yang and *Phoebe zhenman* S. Lee et F. N. Wei seedlings in subtropical China. Forests 7, 78 doi:10.3390/f7040078.

Cohen, J.D., Baldi, B.G., Slovin, J.P., 1986. 13C6-[benzene ring]-indole-3-acetic acid. Plant Physiol. 80, 14-19.

Champigny, M.-L., and Foyer, C.H., 1992. Nitrate activation of cytosolic protein kinases diverts photosynthetic carbon from sucrose to amino acid biosynthesis. Plant Physiol. 100, 7-12.

Chiou, T.J., and Lin, S.I., 2011. Signaling network in sensing phosphate availability in plants. Annu. Rev. Plant Biol. 62, 185-206.

Cotrozzi, L., Remorini, D., Pellegrini, E., Landi, M., Massai, R., Nali, C., et al. 2016. Variations in physiological and biochemical traits of oak seedlings grown under drought and ozone stress. Physiol. Plant. 157, 69-84.

Cotrozzi, L., Pellegrini, E., Guidi, L., Landi, M., Lorenzini, G., Massai, R., et al. 2017a. Losing the warning signal: drought compromises the cross-talk of signaling molecules in *Quercus ilex* exposed to ozone. Front. Plant Sci. 8, 1020, doi: 10.3389/fpls.2017.01020.

Cotrozzi, L., Remorini, D., Pellegrini, E., Guidi, L., Lorenzini, G., Massai, R., et al. 2017b. Cross-talk between physiological and metabolic adjustments adopted by *Quercus cerris* to mitigate the effects of severe drought and realistic future ozone concentrations. Forests 8, 148, doi:10.3390/f8050148.

Domingues, T.F., Meir, P., Feldpausch, T.R., Saiz, G., Veenendaal, E.M., Schrodt, F., et al. 2010. Co-limitation of photosynthetic capacity by nitrogen and phosphorus in West Africa woodlands. Plant Cell. Environ. 33, 959-980.

Dumont, J., Keski-Saari, S., Keinänen, M., Cohen, D., Ningre, M., Kontunen-Soppela, S., et al. 2014. Ozone affects ascorbate and glutathione biosynthesis as well as amino acid contents in three Euramerica poplar genotypes. Tree Physiol. 34, 253-266.

521 Emberson, L.D., Pleijel, H., Ainsworth, E.A., van den Berg, M., Ren, W., Osborne, S., et al. 2018.
522 Ozone effects on crops and consideration in crop models. Eur. J. Agron.
523 doi.org/10.1016/j.eja.2018.06.002.
524 Epstein, E., and Bloom, A.J., 2005. Mineral nutrition of plants: principles and perspectives, Sinauer
525 Ass., Sunderland.
526 Ferretti, M., Marchetto, A., Arisci, S., Bussotti, F., Calderisi, M., Carnicelli, S., et al. 2014. On the
527 tracks of Nitrogen deposition effects on temperate forests at their southern European range-an
528 observational study from Italy. Glob. Chan. Biol. 20, 3423-3438.
529 Foyer, C.H., and Noctor, G. 2011. Ascorbate and glutathione: the heart of the redox hub. Plant
530 Physiol. 155, 2-18.
531 Gao, F., Catalayud, V., Paoletti, E., Hoshika, Y., Feng, Z., 2017. Water stress mitigates the negative
532 effects of ozone on photosynthesis and biomass in poplar plants. Environ. Pollut. 230, 268-279.
533 Gest, N., Gautier, H., Stevens, R., 2013. Ascorbate as seen through plant evolution: the rise of a
534 successful molecule? J. Exp. Bot. 64, 33-53.
535 Gill, S.S., and Tuteja, N., 2010. Reactive oxygen species and antioxidant machinery in abiotic stress
536 tolerance in crop plants. Plant Physiol. Biochem. 48, 909-930.
537 Gottardini, E., Cristofori, A., Cristofolini, F., Nali, C., Pellegrini, E., Bussotti, F., et al. 2014.
538 Chlorophyll-related indicators are linked to visible ozone symptoms: evidence from a field study on
539 native *Viburnum lantana* L. plants in northern Italy. Ecol. Ind. 39, 65-74.
540 Griffith, O.W., 1980. Determination of glutathione and glutathione disulfide using glutathione
541 reductase and 2-vinylpyridine. Anal. Biochem. 106, 207-212.
542 Guidi, L., Remorini, D., Cotrozzi, L., Giordani, T., Lorenzini, G., Massai, R., et al. 2017. The harsh
543 life of an urban tree: the effect of a single pulse of ozone in salt-stressed *Quercus ilex* saplings. Tree
544 Physiol. 37, 246-260.

Harmens, H., Hayes, F., Sharps, K., Mill, G., Calatayud, V., 2017. Leaf traits and photosynthetic responses of *Betula pendula* saplings to a range of ground-level ozone concentrations at a range of nitrogen loads. J. Plant Physiol. 211, 42-52.

Hernández, I., and Munné-Bosch, S., 2015. Linking phosphorus availability with photo-oxidative stress in plants. J. Exp. Bot. 66, 2889-2900.

Hodges, D.M., DeLong, J.M., Forney, C.F., Prange, R.K., 1999. Improving the thiobarbituric acid reactive substances assay for estimating lipid peroxidation in plant tissues containing anthocyanin and other interfering compounds. Planta 207, 604-611.

Hoosbeek, M.R., Lukac, M., van Dam, D., Godbold, D.L., Velthorst, E.J., Biondi, F.A. et al., 2004. More new carbon in the mineral soil of a poplar plantation under Free Air Carbon Enrichment (POPFACE): cause of increased priming effect? Global Biogeochem. Cycles 18, GB1040.

Kampfenkel, K., Van Montagu, M., Inzé, D., 1995. Extraction and determination of ascorbate and dehydroascorbate from plant tissue. Anal. Biochem. 10, 165-167.

Kärenlampi, L., and Skärby, L. (Eds.), 1996. Critical levels for ozone in Europe: testing and finalizing the concepts. UN/ECE Workshop Report. Department of Ecology and Environmental Science. University of Kuopio, Finland, 366 pp.

Kinose, Y., Fukamachi Y., Okabe, S., Hiroshima, H., Watanabe, M., Izuta, T., 2017a. Photosynthetic responses to ozone of upper and lower canopy leaves of *Fagus crenata* Blume seedlings grown under different soil nutrient conditions. Environ. Pollut. 223, 213-222.

Kinose, Y., Fukamachi Y., Okabe, S., Hiroshima, H., Watanabe, M., Izuta, T., 2017b. Nutrient supply to soil offsets the ozone-induced growth reduction in *Fagus crenata* seedlings. Trees 31, 259-272.

Landolt, W., Günthardt-Goerg, M.S., Pfenninger, I., Einig, W., Hampp, R., Maurer, S., et al. 1997. Effect of fertilization on ozone-induced changes in the metabolism of birch (*Betula pendula*) leaves. New Phytol. 137, 389-397.

570 LeBauer, D.S., and Treseder, K.K., 2008. Nitrogen limitation of net primary productivity in
571 terrestrial ecosystems is globally distributed. Ecology 89, 371-379.
572 Lorenzini, G., Guidi, L., Nali, C., Soldatini, G.F., 1999. Quenching analysis in poplar clones
573 exposed to ozone. Tree Physiol. 19, 607-612.
574 Ludwig-Müller, J., Georgiev, M., Bley, T., 2008. Metabolite and hormonal status of hairy root
575 cultures of Devil's claw (*Harpagophytum procumbens*) in flasks and in a bubble column bioreactor.
576 Process Biochem. 43, 15-23.
577 Marzuoli, R., Gerosa, G., Desotgiu, R., Bussotti, F., Ballarin-Denti, A., 2008. Ozone fluxes and
578 foliar injury development in the ozone-sensitive poplar clone Oxford (*Populus maximowiczii* ×
579 *Populus berolinensis*): a dose-response analysis. Tree Physiol. 29, 67-76.
580 Marzuoli, R., Monga, R., Finco, A., Chiesa, M., Gerosa, G., 2018. Increased nitrogen wet
581 deposition triggers negative effects of ozone on the biomass production of *Carpinus betulus* L.
582 young trees. Environ. Exp. Bot. 152, 128-136.
583 Maurer, S., and Matyssek, R., 1997. Nutrition and the ozone sensitivity of birch (*Betula pendula*).
584 Trees 12, 11-20.
585 Neuberg, M., Pavlíková, D., Pavlík, M., Balík, J., 2010. The effect of different nitrogen nutrition on
586 proline and asparagines content in plant. Plant Soil Environ. 56, 305-311.
587 Niu, Y., Chai, R., Dong, H., Wang, H., Tang, C., Zhang, Y., 2012. Effect of elevated CO_2 on
588 phosphorus nutrition of phosphate-deficient *Arabidopsis thaliana* (L.) Heynh under different
589 nitrogen forms. J. Exp. Bot. 64, 355-367.
590 Noctor, G., and Foyer, C.H., 1998. Ascorbate and glutathione: keeping active oxygen under control.
591 Annu. Rev. Plant Physiol. Plant Mol. Biol. 49, 249-279.
592 Pääkkönen, E., and Holopainen, T., 1995. Influence of nitrogen supply on the response of clones of
593 birch (*Betula pendula* Roth.) to ozone. New Phytol. 129, 595-603.

Paoletti, E., Ferrara, A.M., Calatayud, V., Cerveró, V., Giannetti, F., Sanz, M.J., et al. 2009. Deciduous shrubs for ozone bioindication: *Hibiscus syriacus* as an example. Environ. Pollut. 157, 865-870.

Paoletti, E., Materassi, A., Fasano, G., Hoshika, Y., Carriero, G., Silaghi, D., et al. 2017. A new-generation 3D ozone FACE (Free Air Controlled Exposure). Sci. Tot. Environ. 575, 1407-1414.

Pell, E.J., Sinn, J.P., Johansen, V., 1995. Nitrogen supply as a limiting factor determining the sensitivity of *Populus tremuloides* Michx. to ozone stress. New Phytol. 130, 437-446.

Pellegrini, E., Francini, A., Lorenzini, G., Nali, C., 2011. PSII photochemistry and carboxylation efficiency in *Liriodendron tulipifera* under ozone exposure. Environ. Exp. Bot. 70, 217-226.

Pellegrini, E., Cioni, P.L., Francini, A., Lorenzini, G., Nali, C., Flamini, G., 2012. Volatiles emission patterns in poplar clones varying in response to ozone. J. Chem. Ecol., 38, 924-932.

Pellegrini, E., Campanella, A., Paolocci, M., Trivellini, A., Gennai, C., Muganu, M., et al. 2015. Functional leaf traits and diurnal dynamics of photosynthetic parameters predict the behavior of grapevine varieties towards ozone. PlosOne 10, doi:10.1371/journal.pone.0135056.

Pellegrini, E., Trivellini, A., Cotrozzi, L., Vernieri, P., Nali, C., 2016. Involvement of phytohormones in plant responses to ozone. In: Plant hormones under challenging environmental factors, Golam, J.A., Jingquan, Y. (Eds.), Springer, pp. 215-245.

Pellegrini, E., Campanella, A., Cotrozzi, L., Tonelli, M., Nali, C., Lorenzini, G., 2018. What about the detoxification mechanisms underlying ozone sensitivity in *Liriodendron tulipifera*? Environ. Sci. Pollut. Res. 25: 8148-8160.

Pintó-Marijuan M., and Munné-Bosch, S., 2014. Photo-oxidative stress markers as a measure of abiotic stress-induced leaf senescence: advantages and limitations. J. Exp. Bot. 65, 3845-3857.

Polle, A., 1996. Mehler reaction: friend or foe in photosynthesis. Bot. Acta 109, 84-89.

Potvin, C., and Tardif, S., 1988. Sources of variability and experimental designs in growth 655 chambers. Funct. Ecol. 2, 123-130.

619 Plaxton, C.W., and Tran, H.T., 2011. Metabolic adaptations of phosphate-starved plants. Plant
620 Physiol. 156, 1006-1015.
621 Rao, M.V., Koch J.R., Davis, K.R., 2000. Ozone: a tool for probing programmed cell death in
622 plants. Plant Mol. Biol. 44, 345-358.
623 Shang, B., Feng, Z., Li, P., Calatayud, V., 2018. Elevated ozone affects C, N, and P ecological
624 stoichiometry and nutrient resorption of two poplar clones. Environ. Pollut. 234, 136-144.
625 Sharma, P., Jha, A.B., Dubey, R.S., Pessarakli, M., 2012. Reactive oxygen species, oxidative
626 damage, and antioxidative defense mechanisms in plants under stressful conditions. J. Bot. 217037,
627 doi: 10.1155/2012/217037
628 Singh, P., Agrawal, M., Agrawal, S.B., 2009. Evaluation of physiological growth and yield
629 responses of a tropical oil crop (*Brassica campestris* L. var. Kranti) under ambient ozone pollution
630 at varying NPK levels. Environ. Pollut. 157, 871-880.
631 Szabados, L., and Savouré, A., 2010. Proline: a multifunctional amino acid. Trends Plant Sci. 15,
632 89-97.
633 Stevenson, F.J., and Cole, M.A., 1999. Cycles of soil (carbon, nitrogen phosphorus, sulfur,
634 micronutrients). John Wiley and Sons, Hoboken, 427 pp.
635 Tonelli, M., Pellegrini, E., D'Angiolillo, F., Petersen, M., Nali, C., Pistelli, L., et al., 2015. Ozone-
636 elicited secondary metabolites in shoot cultures of *Melissa officinalis* L. Plant Cell Tiss. Organ.
637 Cult. 120, 617-629.
638 Utriainen, J., and Holopainen, T., 2001. Influence of nitrogen and phosphorus availability and
639 ozone stress on Norway spruce seedlings. Tree Physiol. 21, 447-456.
640 van Hove, L.W., Bossen, M.E., San Gabino, B.G., Sgreva, C., 2001. The ability of apoplastic
641 ascorbate to protect poplar leaves against ambient ozone concentrations: a quantitative approach.
642 Environ. Pollut. 114, 371-382.

643 Watanabe, M., Yamaguchi, M., Matsumura, H., Kohno, Y., Izuta, T., 2012. Risk assessment of
644 ozone impact on *Fagus crenata* in Japan: consideration of atmospheric nitrogen deposition. Eur. J.
645 Forest Res., 131, 475-484.
646 Wooliver, R.C., Marion, Z.H., Peterson, C.R., Potts, B.M., Senior, J.K., Bailey, J.K., et al. 2017.
647 Phylogeny is a powerful tool for predicting plant biomass responses to nitrogen enrichment.
648 Ecology 98, 2120-2132.
649 Yang, N., Wang, X., Cotrozzi, L., Chen, Y., Zheng, F., 2016. Ozone effects on photosynthesis of
650 ornamental species suitable for urban green spaces of China. Urban For. Urban Green. 20, 437-447.
651 Zhang, L., Hoshika, Y., Carrari, E., Paoletti, E., 2018a. Ozone risk assessment is affected by
652 nutrient availability: evidence from a simulation experiment under free air controlled exposure
653 (FACE). Environ. Pollut., 238, 812-822.
654 Zhang, L., Hoshika, Y., Carrari, E., Cotrozzi, L., Pellegrini, E., Paoletti, E., 2018b. Effects of
655 nitrogen and phosphorus imbalance on photosynthetic traits of poplar Oxford clone under ozone
656 pollution J. Plant Res., 131, 915-924.

Table 1. Plant Injury Index (PII) on *Populus maximoviczii* Henry × *Populus berolinensis* Dippel (clone Oxford) leaves under free air O_3 exposure [applied for 5 months: ambient air (AA), 1.5 × and 2.0 × ambient O_3 (1.5 × AA and 2.0 × AA)] and subjected to six combinations of nutrient treatment [two levels of N (0 and 80 kg N ha^{-1}; N0 and N80) and three P concentrations (0, 40 and 80 kg P ha^{-1}; P0, P40 and P80)]. Data are shown as mean ± standard deviation. Different letters indicate significant differences among all treatments ($P \leq 0.05$; Tukey's HSD test). Asterisks show the significance of factors/interaction: *** $P \leq 0.001$.

	N0_P0	**N0_P40**	**N0_P80**	**N80_P0**	**N80_P40**	**N80_P80**
AA	3.0±0.56 bc	2.3±0.51 abc	1.6±0.37 ab	1.5±0.06 ab	1.1±0.10 a	1.7±0.20 ab
1.5 × AA	9.5±0.64 gh	5.1±0.12 de	3.0±0.10 bc	3.7±0.31 cd	2.9±0.23 bc	3.5±0.32 c
2.0 × AA	11.1±1.10 h	5.9±0.36 ef	5.1±0.37 de	3.3±0.46 c	7.3±0.92 f	9.4±0.09 g
O_3 ***						
N enrichment ***						
P enrichment ***						
O_3 × N enrichment ***						
O_3 × P enrichment ***						
N enrichment × P enrichment ***						
O_3 x N enrichment × P enrichment ***						

665 Table 2. *P* values of three-way split-plot ANOVA of the effects of O_3, N and P enrichment, and their interactions on malondialdehyde (MDA),
666 superoxide anion radical ($O_2^{\bullet-}$), hydrogen peroxide (H_2O_2), total carotenoids (Tot Car), ascorbate/dehydroascorbate ratio (AsA/DHA), reduced/
667 oxidized glutathione ratio (GSH/GSSG), proline (Pro), abscisic acid/indole-3-acetic acid ratio (ABA/IAA) and water soluble carbohydrate (WSC).
668 Asterisks show the significance of factors/interaction: *** $P \leq 0.001$, ** $P \leq 0.01$; * $P \leq 0.05$; ns $P > 0.05$. d.f. represents the degrees of freedom.

Effects	d.f.	MDA	$O_2^{\bullet-}$	H_2O_2	Tot Car	AsA/DHA	GSH/GSSG	Pro	ABA/IAA	WSC
O_3	2	***	***	***	***	***	***	***	***	***
N enrichment	1	*	ns	***	***	***	***	***	*	***
P enrichment	2	*	***	***	***	***	***	***	ns	***
O_3 × N enrichment	2	***	***	***	***	***	***	***	*	***
O_3 × P enrichment	4	***	***	***	***	***	***	***	***	***
N enrichment × P enrichment	2	***	***	***	***	***	***	***	***	***
O_3 × N enrichment × P enrichment	4	***	***	***	***	***	***	***	***	**

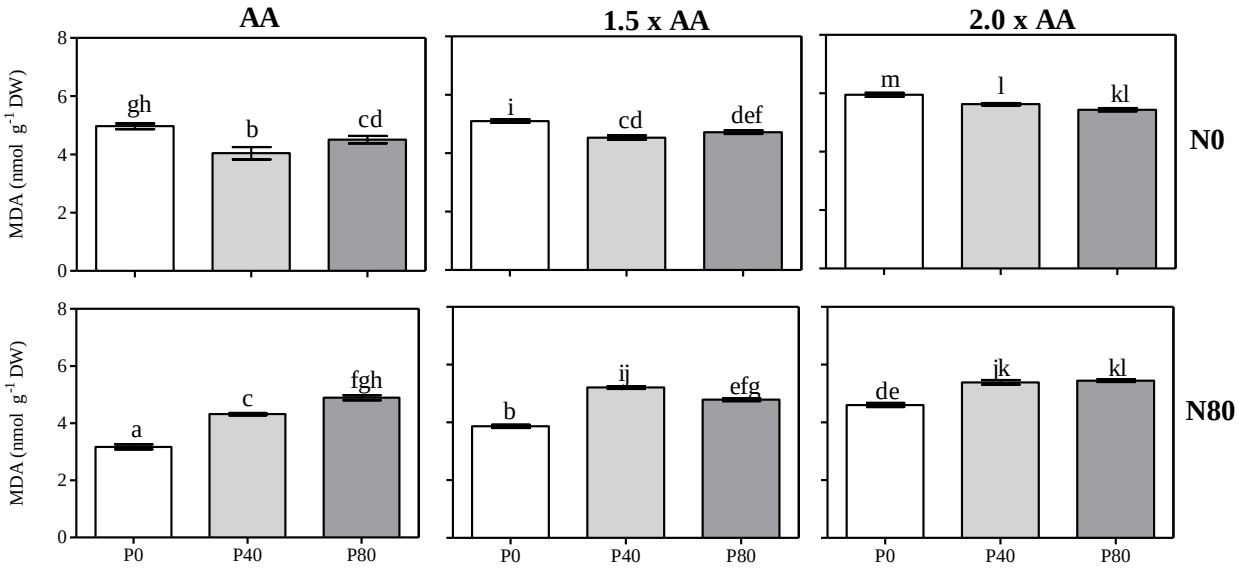

669
670

671 Fig. 1. Quantification of malondialdehyde (MDA) by-product in *Populus maximoviczii* Henry ×
672 *Populus berolinensis* Dippel (clone Oxford) leaves under free air O_3 exposure [applied for 5
673 months: ambient air (AA), 1.5 × and 2.0 × ambient O_3 (1.5 × AA and 2.0 × AA)] and subjected to
674 six combinations of nutrient treatment [two levels of N (0 and 80 kg N ha^{-1}; N0 and N80) and three
675 P concentrations (0, 40 and 80 kg P ha^{-1}; P0, P40 and P80)]. Data are shown as mean ± standard
676 deviation. Different letters indicate significant differences among all treatments ($P \leq 0.05$; Tukey's
677 HSD test; N = 3; see Table 2); DW, dry weight.

678

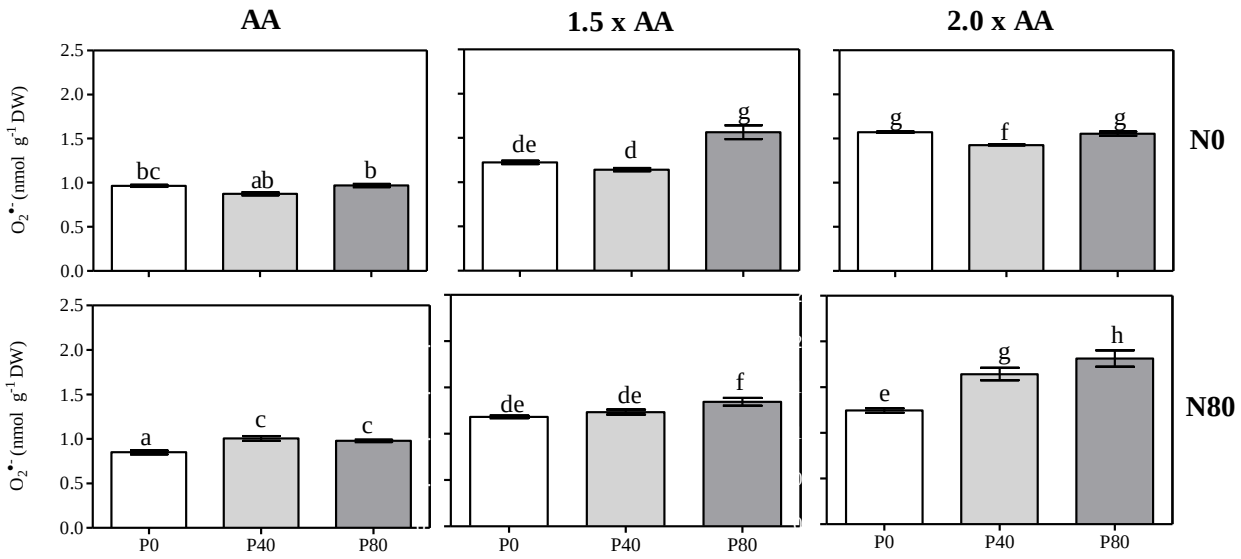

679
680

681 Fig. 2. Quantification of superoxide anion radical ($O_2^{\bullet-}$) in *Populus maximoviczii* Henry × *Populus*
682 *berolinensis* Dippel (clone Oxford) leaves under free air O_3 exposure and subjected to six
683 combinations of nutrient treatment. For details, see Figure 1. Data are shown as mean ± standard
684 deviation. Different letters indicate significant differences among all treatments ($P \leq 0.05$; Tukey's
685 HSD test; N = 3; see Table 2).

686

687

688

689

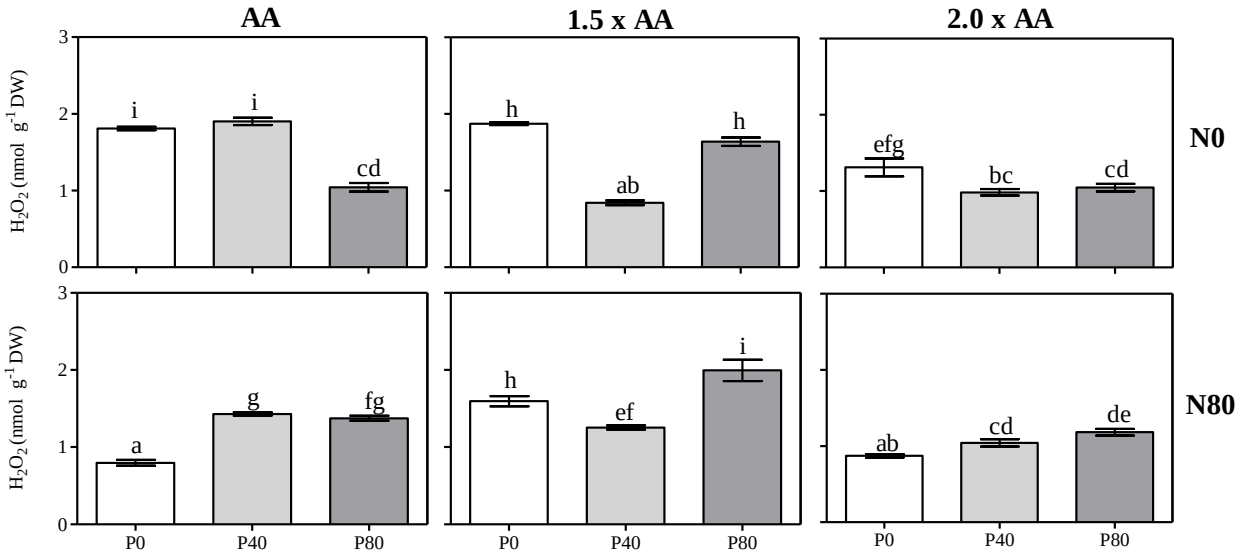

Fig. 3. Quantification of hydrogen peroxide (H_2O_2) in *Populus maximoviczii* Henry × *Populus berolinensis* Dippel (clone Oxford) leaves under free air O_3 exposure and subjected to six combinations of nutrient treatment. For details, see Figure 1. Data are shown as mean ± standard deviation. Different letters indicate significant differences among all treatments ($P \leq 0.05$; Tukey's HSD test; N = 3; see Table 2).

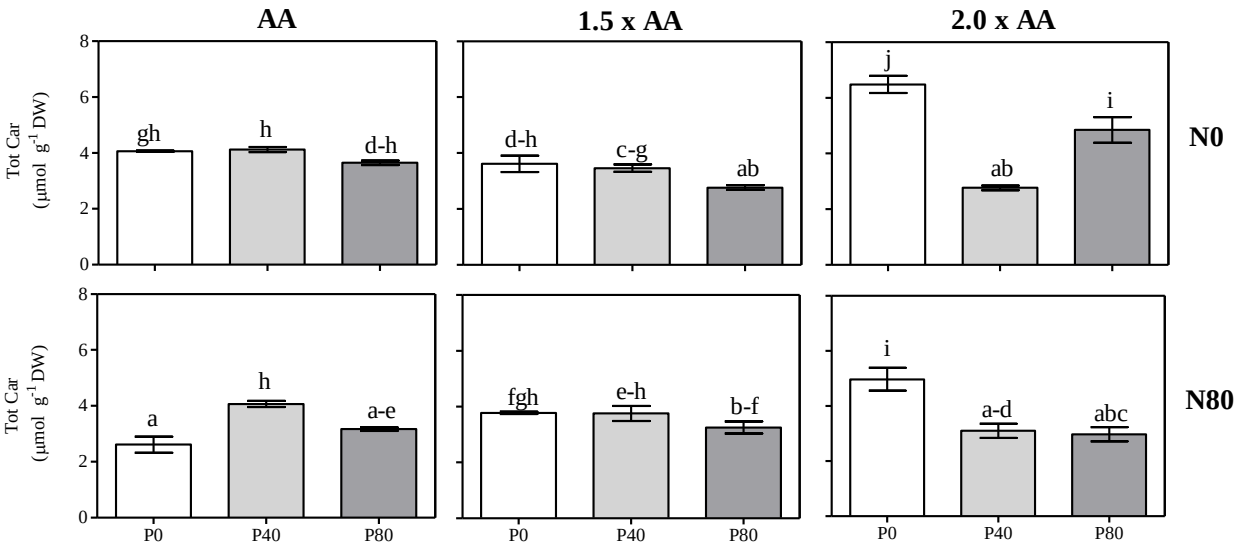

Fig. 4. Quantification of total carotenoids (Tot Car) in *Populus maximoviczii* Henry × *Populus berolinensis* Dippel (clone Oxford) leaves under free air O_3 exposure and subjected to six combinations of nutrient treatment. For details, see Figure 1. Data are shown as mean ± standard deviation. Different letters indicate significant differences among all treatments ($P \leq 0.05$; Tukey's HSD test; N = 3; see Table 2).

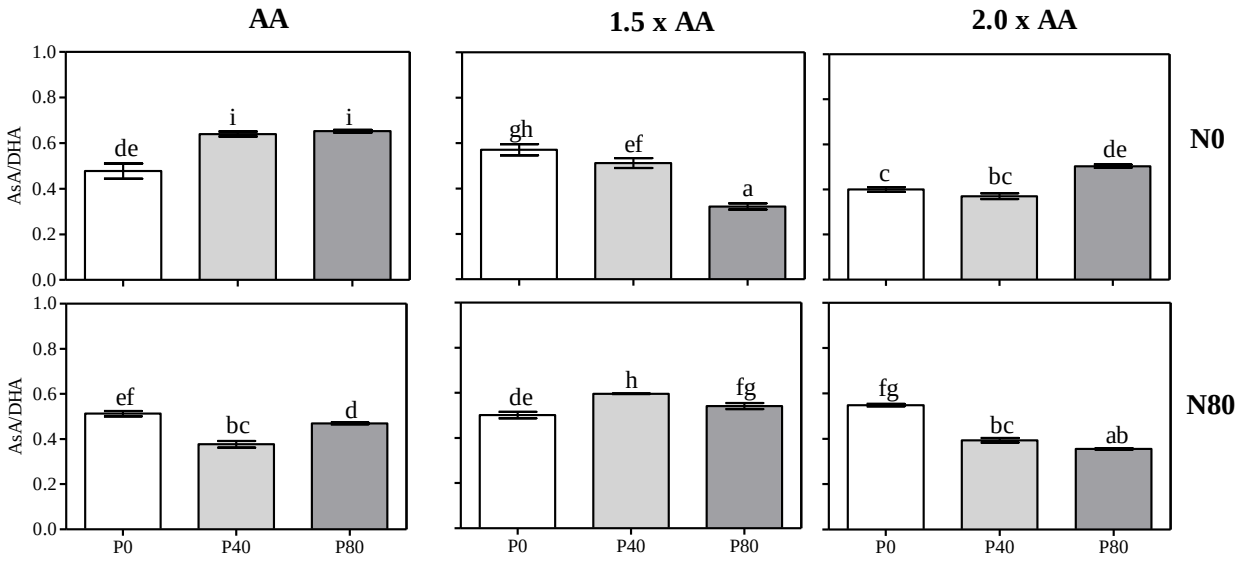

708

709 Fig. 5. Quantification of ascorbate/dehydroascorbate ratio (AsA/DHA) in *Populus maximoviczii*
710 Henry × *Populus berolinensis* Dippel (clone Oxford) leaves under free air O_3 exposure and
711 subjected to six combinations of nutrient treatment. For details, see Figure 1. Data are shown as
712 mean ± standard deviation. Different letters indicate significant differences among all treatments (P
713 ≤ 0.05; Tukey's HSD test; N = 3; see Table 2).

714

715

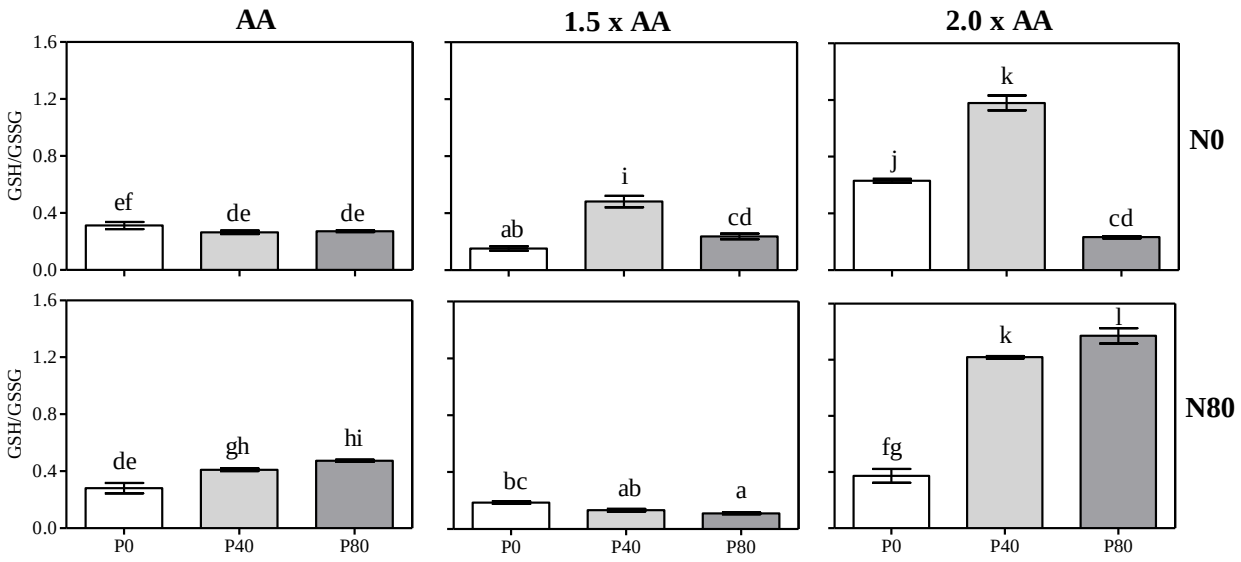

716

717 Fig. 6. Quantification of reduced/oxidized glutathione ratio (GSH/GSSG) in *Populus maximoviczii*
718 Henry × *Populus berolinensis* Dippel (clone Oxford) leaves under free air O_3 exposure and
719 subjected to six combinations of nutrient treatment. For details, see Figure 1. Data are shown as
720 mean ± standard deviation. Different letters indicate significant differences among all treatments (P
721 ≤ 0.05; Tukey's HSD test; N = 3; see Table 2).

722

723

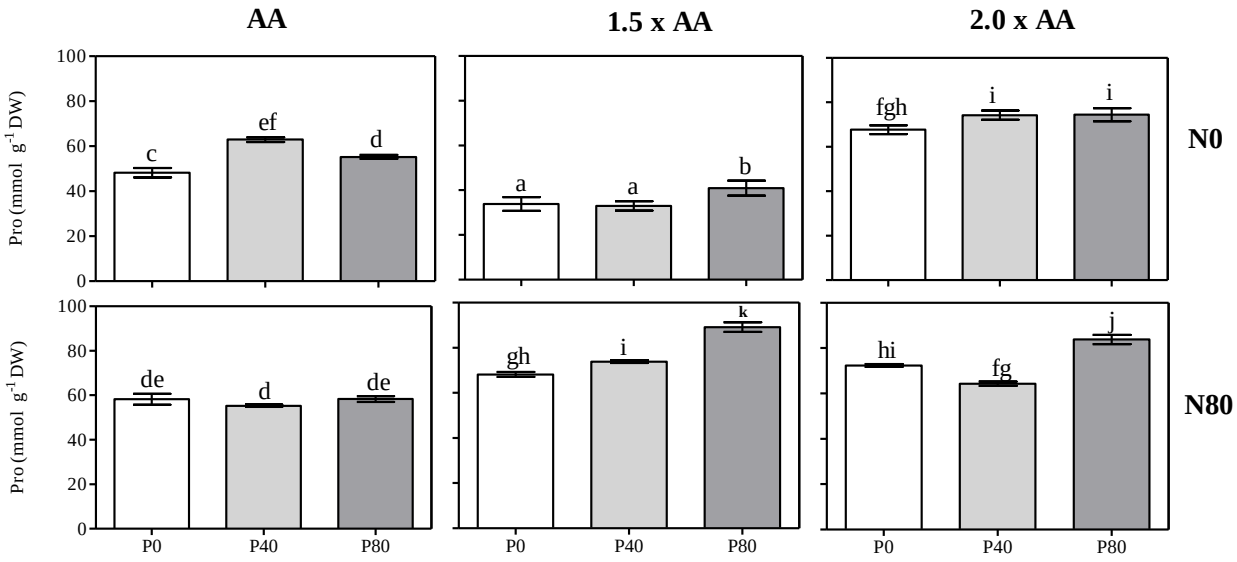

724

725 Fig. 7. Quantification of proline (Pro) in *Populus maximoviczii* Henry × *Populus berolinensis*
726 Dippel (clone Oxford) leaves under free air O_3 exposure and subjected to six combinations of
727 nutrient treatment. For details, see Figure 1. Data are shown as mean ± standard deviation. Different
728 letters indicate significant differences among all treatments ($P \leq 0.05$; Tukey's HSD test; N = 3; see
729 Table 2).

730

731

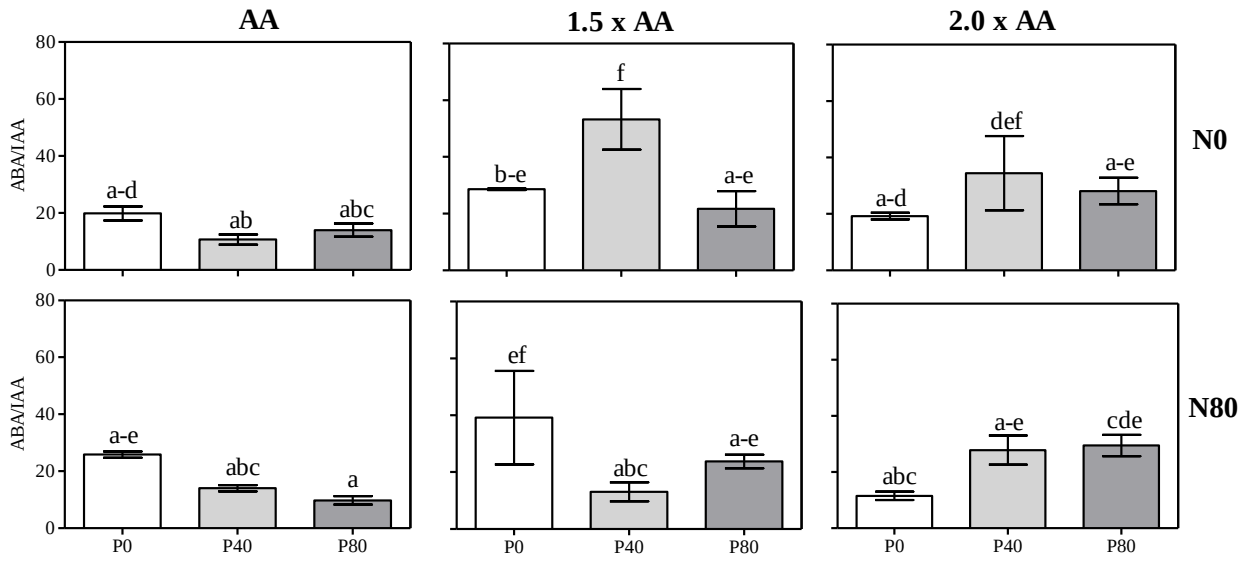

732

733 Fig. 8. Quantification of abscisic acid/indole-3-acetic acid ratio (ABA/IAA) in *Populus*
734 *maximoviczii* Henry × *Populus berolinensis* Dippel (clone Oxford) leaves under free air O_3
735 exposure and subjected to six combinations of nutrient treatment. For details, see Figure 1. Data are
736 shown as mean ± standard deviation. Different letters indicate significant differences among all
737 treatments ($P \leq 0.05$; Tukey's HSD test; N = 3; see Table 2).

738

739

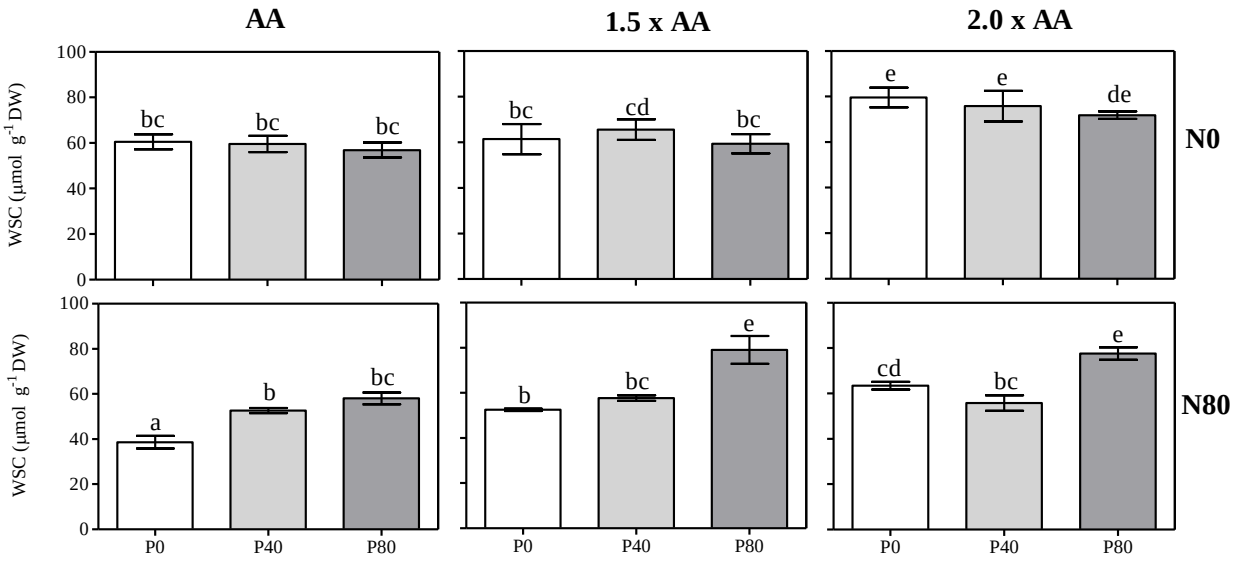

740

741 Fig. 9. Quantification of water soluble carbohydrates (WSC) in *Populus maximoviczii* Henry ×
742 *Populus berolinensis* Dippel (clone Oxford) leaves under free air O_3 exposure and subjected to six
743 combinations of nutrient treatment. For details, see Figure 1. Data are shown as mean ± standard
744 deviation. Different letters indicate significant differences among all treatments ($P \leq 0.05$; Tukey's
745 HSD test; N = 3; see Table 2).

746

747